The International Journal of Advanced Manufacturing Technology (2023) 128:611–623
https://doi.org/10.1007/s00170-023-11856-6

ORIGINAL ARTICLE

Ball-end micro-milling of material measures: wear behavior in field use

Katja Klauer-Dobrowolski[1] · Matthias Eifler[2,3] · Benjamin Kirsch[1] · Jörg Seewig[2] · Jan C. Aurich[1]

Received: 9 February 2023 / Accepted: 27 June 2023 / Published online: 16 July 2023
© The Author(s) 2023

Abstract
Micro-millingis a precise method for micro-structuring component surfaces. When complex or free-form structures like material measures are to be manufactured, ball-end milling tools are particularly suitable. In preliminary studies by the authors, areal material measures for the calibration of optical topography measuring instruments were manufactured via micro-milling. The demands on the surface quality of the material measures are extremely high. Therefore, worn tools must not be used if the wear has a direct effect on the resulting topography of the manufactured material measures. At the same time, the micro-milling tools used are very costly and should therefore be used as long as possible. A comprehensive experimental study was carried out on the wear behavior of different ball-end micro-milling tools for the specific use case of areal material measures. In the investigations, brass CuZn39Pb3 was machined and different areal material measures were manufactured. The tool life dependent wear was determined and critical wear was identified.

Keywords Micro-milling · Ball-end milling tool · Wear behavior

1 Introduction and state of the art

Optical measuring instruments must be calibrated to estimate their measurement uncertainty and allow a traceability of the measurement with regard to the basic unit of length. For calibration, the measurement of a material measure which images a defined quantity value of the measurand needs to be performed. Thus, the requirements for the manufacturing of material measures are high. In previous studies by other authors—Nemoto et al. performed a first study [1] and Leach et al. by combining the process with a replication using electroforming [2]—it was shown that micro-milling can be used as a suitable process for the manufacturing of material measures.

✉ Matthias Eifler
meifler@rptu.de

[1] Institute for Manufacturing Technology and Production Systems, RPTU Kaiserslautern-Landau, Gottlieb-Daimler-Str., 67663 Kaiserslautern, Germany

[2] Institute for Measurement and Sensor-Technology, RPTU Kaiserslautern-Landau, Gottlieb-Daimler-Str., 67663 Kaiserslautern, Germany

[3] IU University of Applied Sciences, Juri-Gagarin-Ring 152, 99084 Erfurt, Germany

Material measures must feature very high surface qualities and dimensional accuracy. Therefore, the milling process must be well understood with regard to systematic effects and independent of stochastic influences. A process design has already been carried out by the authors [3]. Various process parameters and control dataset parameters were investigated.

However, also, tool wear can lead to deviations, which must be considered and investigated separately. When using very expensive micro-milling tools, especially diamond tools (costs > 1000 €), they must be used as long as possible to assure an economically productive process. In addition, the use of the maximum tool life also leads to an increase in the sustainability of the process. At the same time, tool wear must not become too high to not negatively affect the manufactured surface, because otherwise the material measures cannot be used, which will again reduce the productivity. Therefore, for the described application, it must be precisely and particularly examined at which tool life travel path critical tool wear is to be expected and the tool must be changed.

Due to the complexity of tool wear, especially due to the different wear types [4], a multitude of different measuring methods are used for the assessment [5]. The methods for the wear investigation of tools can be categorized as in-line systems or measuring systems that interrupt the process. Another distinction can be made between direct and indirect measuring

systems [6]. Cheng summarized the methods for wear monitoring in micro-cutting with scanning electron microscopy (SEM) for process interruption and cutting force, burr size, and acoustic measurement for in-line measurement [7]. Zhang and Zhang described a wear monitoring system for ball-end micro-milling based on machine vision [8], Fernández-Robles et al. also applied methods originating from image processing [9], Li described the utilization of acoustic methods [10], and Byrne et al. provided an overview of the different possibilities for tool condition monitoring [11]. Malekian et al. implemented a multi-sensor approach for micro-milling using accelerometers, force, and acoustic sensors [12] and Oliaei analyzed the relation between tool wear and the cutting forces [13]. For general milling procedures, Lamraoui et al. used vibration signals for the analysis of tool wear [14] and Stavropoulos et al. described a method based on acceleration and spindle drive where the vibration's signal energy was identified as particularly relevant parameter [15]. Niu et al. performed an examination based on the measurement of cutting forces in micro-milling processes [16]. Zhang et al. introduced a modeling approach for the surface generation including the description of tool wear and its influence on the resulting surface topography [17]. In another publication, the stochastic tool wear progression model was used to optimize micro-milling processes with regard to their energy consumption [18] and the model was further enhanced to predict the occurrence of tool wear and verified experimentally [19]. Zhu et al. also used the cutting forces to determine the tool wear based on a multi-category classification approach [20]. Alhadeff et al. provided a protocol for the measurement of tool wear in micro-milling and experimentally examined its application for the materials brass, titanium, and Hastelloy [21]. Rahman et al. also used the cutting forces as initial point for the determination of tool wear and failure mechanisms in micro-milling [22]. Zhu and Yu used a different approach and estimated the tool wear in micro-milling processes based on morphological component analysis [23]. Schaller et al. carried out wear tests in brass using cemented carbide micro-milling tools [24]. The study of Schaller et al. [24] therefore served as the basis for designing the wear study described in this publication. However, only the initial wear (see I in Fig. 1) or its effect on the resulting surface quality is relevant for the manufacturing of material measures. Therefore, in contrast to the study of Schaller et al. [24], in which feed travels of more than 10 m were investigated, this study focuses on the investigation of shorter feed travel.

Based on the state of the art including the given references, it can be stated that the tool wear in micro-machining processes has been examined for different processes including micro-milling, and possible monitoring methods have been compared and possible solutions outlined. The subsequently presented study aims at describing the effect of tool wear for the specific application of micro-milling of areal material measures which feature complex structures. As already described, areal material measures must feature high-precision surfaces, which is why the quality requirements are significantly higher than for other micro-components. The manufacturing of areal material measures is therefore a special case that clearly differs in its requirements from other micro-components. For the examination, the typical state-of-the-art measurement methods are used and compared in order to determine which methods are best suitable for the given application.

Different tools and different target geometries are investigated based not only on the topography information, but also the process force and scanning electron microscopy. After evaluating these results and combining the information obtained with the measurement methods, it can be concluded which of the individual methods is particularly suitable for the early detection of wear on micro-milling tools.

2 Experimental setup

2.1 Machining setup

The tests were performed on a LT Ultra MMC 600H* machine tool (see Fig. 2). Two different tools were tested which differ in almost all of their properties (see Fig. 3), to determine the robustness of the wear detection. It will also be examined if the wear has to be detected on the basis of SEM images of the tool or if an in situ force measurement can be used to detect wear before a notable deviation of the defined surface texture parameters of the material measures occurs.

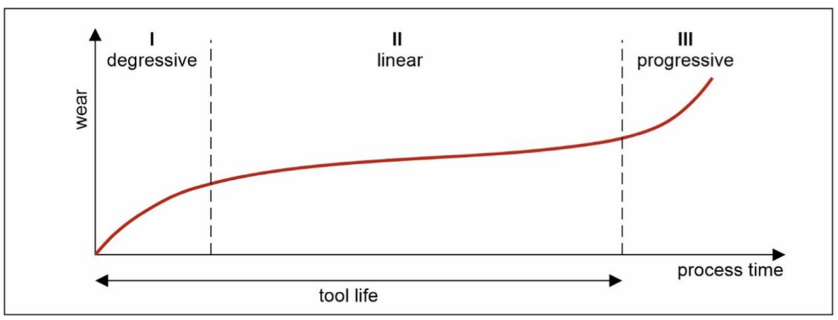

Fig. 1 Tool wear over process time according to [25]

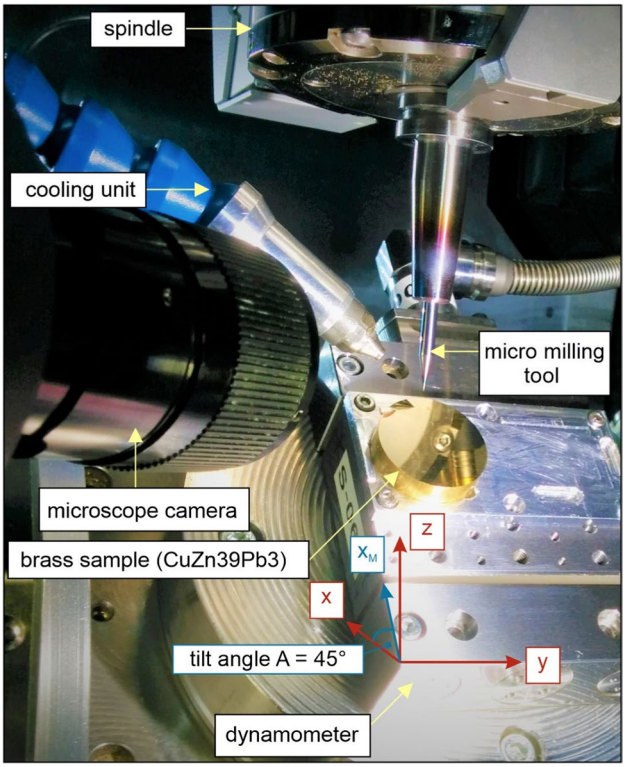

Fig. 2 Machine tool and coordinate system

Two material measures were manufactured for wear investigation, which feature a profile-based geometry and thus have constant height values in the x_M-direction (for machine coordinate system, see Fig. 2). A meander-shaped tool path was proven in a separate study to combine the highest time efficiency with consistently good surface qualities [26].

Due to this meander-shaped tool path (see Fig. 4), wear can also be detected within the individual structured calibration areas: Each calibration field is manufactured by adjacent tool paths in x_M-direction. Ideally, these paths look identical—without occurrence of tool wear. Changes of the surface topography that can be observed between the individual paths within a field with increasing x_M would be an indicator of increasing tool wear during the manufacturing of one field.

The structures were manufactured in brass $CuZn_{39}Pb_3$, since this workpiece material is also used for real material measures. Brass is easy to machine and suitable for optical measurements due to its optical cooperativeness.

2.2 Experimental design

The process parameters were based on various preliminary studies by the authors and chosen as summarized in Table 1. A tilt angle of 45° was set between the tool and the workpiece during manufacturing. This is common when using ball-end milling tools to avoid a contact with the area of the tool where the cutting speed, which varies with the radius, is zero. With the machine tool used, it is not possible to tilt the tool, so the workpiece was tilted. The control dataset was adapted to take this inclination into account during manufacturing (see Fig. 2).

The definition of the feed travel which was investigated in this study was done based on the results of previous studies from other authors (see Sect. 1, e.g. [1]). To estimate the expected wear for the AFL and PPS geometries, the

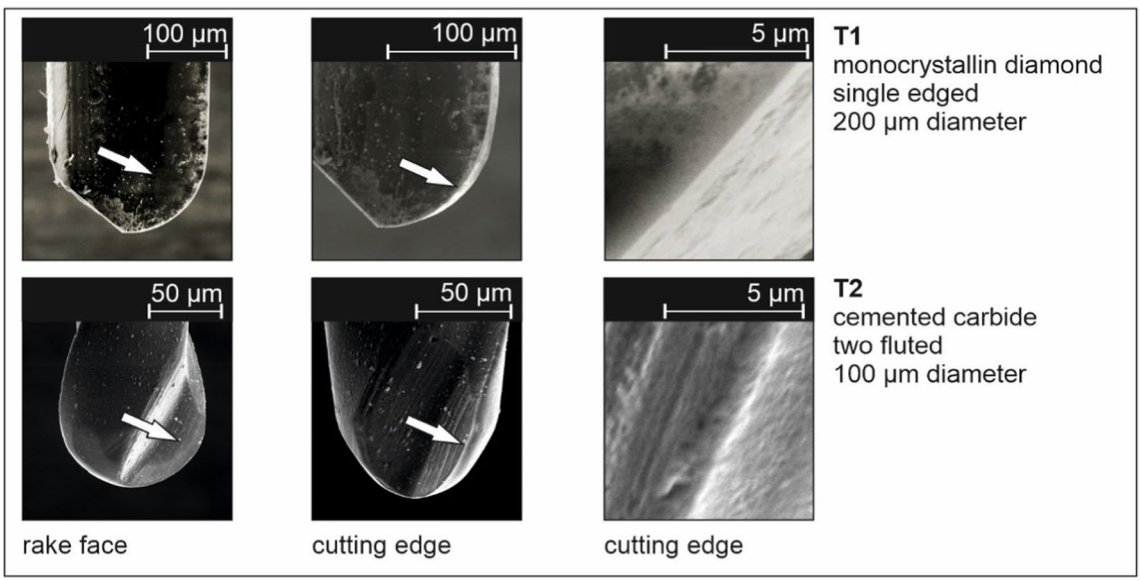

Fig. 3 Tested tools [3]

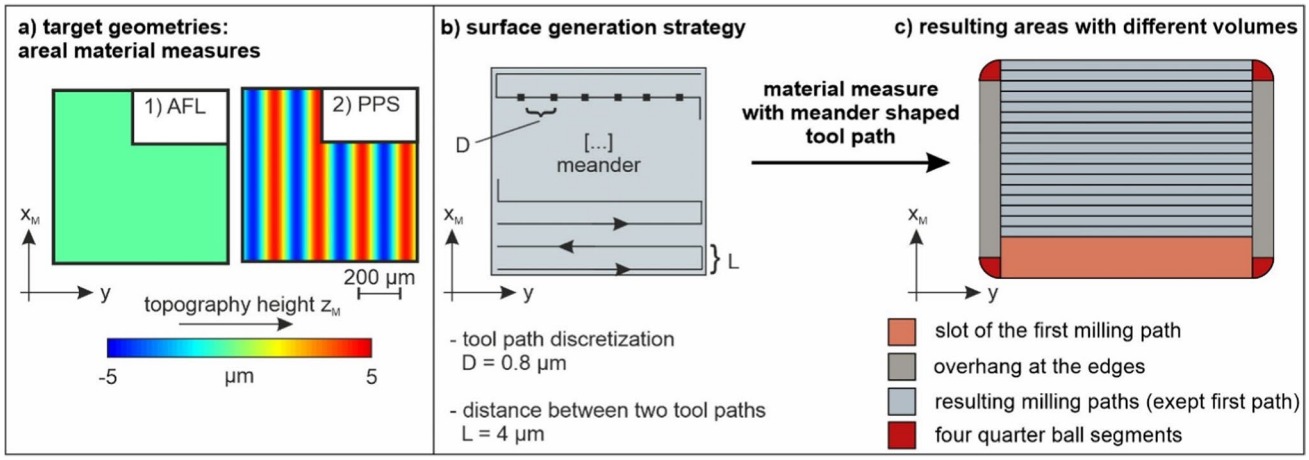

Fig. 4 Target geometries and surface generation according to [3, 27]

Table 1 Process parameters during micro-milling [3]

Parameters			Value or setup
Target geometries			AFL and PPS, according to [28]
Tools			T1 ($R = 100$ µm) T2 ($R = 50$ µm)
Control dataset parameters		Distance between two tool paths, L (µm)	4
		Discretization D, (µm)	0.8
		Tilt angle, A (°)	45
Cutting parameters	T1	Spindle speed, n (rpm)	18,000
		Feed rate, v_f (mm/min)	4.5
	T2	Spindle speed, n (rpm)	18,000
		Feed rate, v_f (mm/min)	9
Surface generation			Meander-shaped tool path (alternating feed travel)

nominal, undeformed material removal based on geometric conditions was calculated (see Table 2 with the parameters for the manufacturing of each material measure, each single slot and the overall study).

As shown in Fig. 4, the manufactured geometries include the type AFL (areal flat surface) geometry and the type PPS (profile periodic sinusoidal) geometry, both standardized in ISO 25178–70 as material measures. Additionally, all tools were used to manufacture single slots to perform a process force measurement (see Table 3). A force measurement during the manufacturing of the material measures is not feasible for calculating integral residual force values, because the directional changes in the meandering feed path result in peaks in the force signal, which are caused by the inertia of the axis and do not represent the actual process forces. Hence, in addition to the material measures, individual slots were manufactured where the process forces were measured.

The material removal was also calculated for the single slots with a length of 5 mm and a cutting depth of 7.071 µm. The cutting depth results from the infeed of 10 µm in z-direction. On the inclined workpiece, this results in a cutting depth of 7.071 µm perpendicular to the workpiece surface.

For the study, based on the estimation of Table 3, 15 material measures and four single slots were examined as total feed travel. The result is a total feed travel of approx. 3.4 to 3.5 m within the individual studies.

While the process force can be measured during the milling process, but only for the milling of the slots, not for the milling of the material measures, the SEM images and the measured surface topography by confocal microscopy can only be taken with process interruption. Hence, a special design of experiments (test order) was necessary that combined the described requirements (see Table 3). Since the SEM images are very time-consuming, they were only provided at four points in the experimental plan: before the test run (new tool, without wear), after test 1, after test 2, and after test 3.

Tests 1–3 consisted of a predefined routine and order of the manufactured slots and material measures with each tool (see

Table 2 Feed travel and nominal, undeformed material removal for the different tools and material measures [3]

	AFL		PPS
	T1	T2	T2
Material measures			
Feed travel, l_v (µm)	227,528	227,528	230,295 (227,528 projected path)
Cutting depth, a_p (µm)	6.093	6.093	6.093 (zero crossing)
Cross-section of undeformed chip of the first slot, A_{s1} (µm^2)	280.969	196.812	196.812 (for zero crossing)
Cross-section of undeformed chips of all other slots, A_s (µm^2)	24.344	24.318	24.318 (for zero crossing)
Material removal, V_w (µm^3)	6,046,133	5,871,739	5,871,739
Single slots (force measurement)			
Feed travel, l_v (µm)	5000	5000	5000
Cutting depth, a_p (µm)	7.071	7.071	7.071
Cross-section of undeformed chip, A_{s1} (µm^2)	350.771	245.321	245.321
Material removal, V_w (µm^3)	1,769,192	1,234,090	1,234,090
Total (15 material measures + 4 slots)			
Feed travel, l_v (µm)	3,432,920	3,432,920	3,474,437
Material removal, V_w (µm^3)	**97,768,763**	**93,012,445**	**93,012,445**

Table 3 Order of tests and nomenclature [1]

	Order of the test (chronological listing)	Nomenclature
Test 1	Single slot	S1
	Material measure	MM1
	Single slot	S2
Test 2	Seven material measures	MM2, MM3, …, MM8
	Single slot	S3
Test 3	Seven material measures	MM9, MM10, …, MM15
	Single slot	S4

Table 3). Within test 1, the initial wear was closely examined. In tests 2 and 3, the remaining tool life was examined in a divided manner. Each test ended with the manufacturing of a single slot to be able to determine the forces in dependence of the wear condition.

Two tools of type T2 (cemented carbid, two fluted) were used: one for the manufacturing of the AFL geometries and one to manufacture the PPS geometries. From type T1, only one tool was used to manufacture the AFL geometries (see Table 3).

3 Measurement and evaluation

Different process parameter values were set and various process result parameters were evaluated to acquire information about the tool wear. For the evaluation, not only the measurement principle of scanning electron microscopy (SEM) was used to acquire images of the tool and the workpiece, but also the topography of the material measures was sampled using a confocal microscope, and the process force was measured in situ (see Sect. 2.2).

3.1 Force measurement and evaluation

The process forces were recorded using a Kistler 9119AA2* dynamometer. The sampling rate of the measuring system was set to 12 kHz for all channels (three channels corresponding to the three spatial directions). The evaluation of the process forces was carried out in Matlab*.

The force evaluation followed the procedure described by Reichenbach [29]: Since some different effects, which are described in the following, have to be considered, a comparison of the raw signal is not reasonable. A detailed description of the evaluation routine as well as diagrams of the force value curves after the corresponding filter steps is shown in the work of Reichenbach [29].

The dynamometer, on which the brass samples were clamped, was rotated by the inclination of the B-axis (see Sect. 2.1). The recorded forces correspond to the passive force F_p (force in the z_M-direction), the feed force F_f (force in the y-direction), and the feed normal force F_{fN} (force in the x_M-direction).

The unfiltered raw signals of the force measurements contained measurement noise and drift. Measurement noise and long-wave components (caused by drift) were removed via the evaluation routine:

The force measurement was already started before tool engagement, so there is an offset at the beginning of the measurement, which was subtracted first. The remaining force signal (tool in contact) was then filtered with a bandpass filter to remove measurement noise and drifts. The bandpass filters frequencies in the range of the frequency of the spindle, since this is the only relevant range for forces resulting directly from the process. Filtering was done in an interval from ($f_s - 50$ Hz) to ($f_s + 50$ Hz), where f_s is the frequency of the spindle for a speed of 18,000 rpm equal to 300 Hz. After filtering, the

process force (total force) for each time point i was calculated from the three directional components:

$$F_{\text{process,i}} = \sqrt{F^2_{\text{x}_\text{M},\text{i}} + F^2_{\text{y,i}} + F^2_{\text{z,i}}} \quad (1)$$

From this time-dependent total force, a mean value F_{process} and an empirical standard deviation std(F_{process}) were then calculated for the complete tool engagement (5 mm feed path per slot).

In general, the value of the standard deviation in milling due to the interrupted cut (change in the direction of force vectors) is high in this evaluation method. However, by directly comparing the standard deviation in the different individual slots, conclusions can still be drawn about wear if the absolute value of the standard deviation shows significant differences. If the standard deviation is significantly higher in one of the slots, it is to be expected that the force signal will show variations within the individual slot, which cannot be explained by the change in direction of the force. In this case, for example, built-up edges or tool breakouts at the cutting edge can be the reason for these variations. However, to draw more precise conclusions, all measurement results from all measurement methods must be considered.

3.2 Confocal microscope and surface texture parameters

To acquire surface topography data, a Nanofocus µsurf explorer* confocal microscope was used with a 20× magnification objective and numerical aperture (NA) of 0.6. This microscope has a nominal vertical resolution in the nanometer range and a spacing of 1.6 µm in the lateral direction when using the mentioned objective. The following routine was applied to evaluate integral surface texture parameters:

First, the measured dataset was aligned and an evaluation area of 600 µm × 600 µm was extracted in the center of the single measurement field. This central evaluation area guarantees that no burr or other edge effects, which are caused for example by path changes during meander-shaped milling strategy, influence the evaluated parameters. A plane was fitted into the dataset using the least-squares method. The fitted plane was then subtracted from the dataset. Subsequently, filtering was performed using a linear areal Gaussian filter according to ISO 16610–61 [30] with a nesting index of 0.8 mm. This filter was used to remove long-wavelength components that may not have been completely removed by fitting the plane. After the measured topography was aligned and the relevant wavelengths were extracted by the two methods described (plane fitting and Gaussian filter), the surface texture parameters Sa and Sq were calculated according to [31].

Each manufactured material measure was measured repetitively four times with the mentioned confocal microscope. An arithmetical mean value and an empirical standard deviation were calculated for the surface texture parameters from each set of four measurements.

3.3 Scanning electron microscope (SEM)

Scanning electron microscope images were taken to qualitatively investigate the geometry and topographical features of the micro-milling tools used. A Philips XL 40* SEM was used for this purpose. The secondary electron detector (SE detector) was used for all images taken for this work. The high voltage was 10 kV. The emission current was set in the range between 50 and 90 µA.

For micro-milling tools, no standardized procedure exists for the quantitative evaluation of tool wear based on microscope images. For the evaluations within this study, this was also omitted, since different cutting materials were used, which cause different optical effects during the SEM measurement. Taking these effects into account, however, a qualitative evaluation is possible.

4 Results

4.1 Resultant forces

The process forces are shown in Table 4 and are considered separately for the different tools.

For tool T1, the resultant forces increase after the slot S2, i.e., after test 1 as described in Table 3 has been conducted. However, the increase is only in the Millinewton range and only insignificantly larger than the measurement noise of the dynamometer, which is why it is essential to verify the increase of wear using the other measurement methods (SEM and surface topography). For the slots S1 and S2 that are manufactured during the first test, the resultant force and its standard deviation are identical, which is why no significant wear is assumed to occur within the manufacturing of the first material measure. Overall, the changes in the standard deviation are very small, which is why no noticeable wear (for example tool breakouts) is to be expected. Based on the force signals, it can be assumed that slight abrasive wear occurs from S3 (after the second test, i.e., overall a manufacturing of eight material measures), but this is negligible for the number of fields investigated in this study.

For tool T2, the resultant force already increases between the manufacturing of the first slot S1 and the second slot S2, i.e., during the machining of the first material measure. This trend is visible for both geometries (AFL and PPS) and the increase continues for both types of material measures AFL and PPS during the second test which includes a manufacturing of another seven material measures before the slot S3 is machined and the next force measurement takes place. For the AFL geometry, the trend continues during the third test after which the slot S4 is machined and another force measurement is performed. In contrast, for the PPS geometry, a decrease in resultant force takes place between the slots S3 and S4 that were manufactured before and after the third test. The

Table 4 Measured resultant forces for different tools and geometries [1]

Tool and geometry	Slot number	Resultant force, $F_{process}$ (N)	Empirical standard deviation of resultant force, std($F_{process}$) (N)
T1, AFL	S1	0.027	0.014
	S2	0.027	0.014
	S3	0.034	0.016
	S4	0.039	0.019
T2, AFL	S1	0.045	0.019
	S2	0.049	0.019
	S3	0.059	0.022
	S4	0.063	0.024
T2, PPS	S1	0.050	0.023
	S2	0.053	0.023
	S3	0.059	0.025
	S4	0.046	0.018

systematic increase suggests abrasive wear, which is continuously evolving. The decrease in resultant force for the PPS geometry probably indicates a change of geometry at the cutting edge. This may be due to the formation or detachment of built-up edges or to a breakout at the cutting edge.

The resultant force values over the tool life are different for the PPS geometry than for the AFL geometry. When comparing the force curves, the varying cutting depths for the PPS geometry must be considered. The varying cutting depths also change the engagement conditions between the two geometries. Furthermore, it is noticeable that for the AFL geometry, the process forces for tool T2 are greater than for tool T1. These differences are mainly due to the different cutting edge radii of the two tools.

4.2 Surface quality

The surface quality is evaluated with the described areal surface texture parameters that are calculated for each manufactured material measure in order to monitor whether changes of the manufactured surface occur due to the progressing tool wear. Whereas the slots serve for the measurement of the process force, the areal surface texture parameters of the manufactured 15 material measures are the measurand that can be used to determine the quality of the manufactured material measures. The evaluated parameters based on four repetitive measurements each do not show any systematic changes with increasing feed travel for tool T1 (see Fig. 5). For the surface texture parameters, there are only changes in the low single-digit nanometer range or, in a few cases, in the low double-digit nanometer range over the entire tool life. This order of magnitude of deviations also corresponds to the resolution limit of the confocal microscope featuring the objective used (see Sect. 3.2). Due to the fact that the overall roughness of the resulting surface topography is in the value range of 15–21 nm for Sa, it can be assumed that the tool wear that has occurred only slightly affects the topography of the material measures since a slight change of the amplitude distribution of the surface would already notably alter the examined surface texture parameters. The quality of the material measures is not negatively affected after 15 manufactured material measures for tool T1. The standard deviations feature values between 0 and 1 nm for T1, AFL; 0–7 nm for T2, AFL; and 0–4 nm for T2, PPS. All values of the standard deviations can be found in the Appendix.

The different progresses for the manufacturing of the type AFL and PPS material measures indicate that for the tool T2, the course of the surface texture parameter values over the feed travel is clearly dependent on the geometry manufactured. Thus, the effects are described individually for both geometries.

4.2.1 T2, AFL

First, the surface texture parameter values decrease and then increase. The increase is particularly strong after the twelfth material measure. The increasing tool wear has a clear effect on the surface texture parameters: The deviations are in the high two- or even three-digit nanometer range. These strong deviations both lie above the resolution limit and measurement uncertainty of the confocal microscope and can thus be interpreted as systematic influences. Accordingly, the occurring tool wear must be considered when manufacturing material measures and a maximum number of 12 type AFL material measures should be manufactured before replacing the tool.

4.2.2 T2, PPS

Sa and Sq show a plateau-like almost constant range after ten manufactured material measures. The combined consideration of the force signal curve and the course of the surface texture parameters over the feed travel leads to the assumption that built-up edges between test 2 and test 3

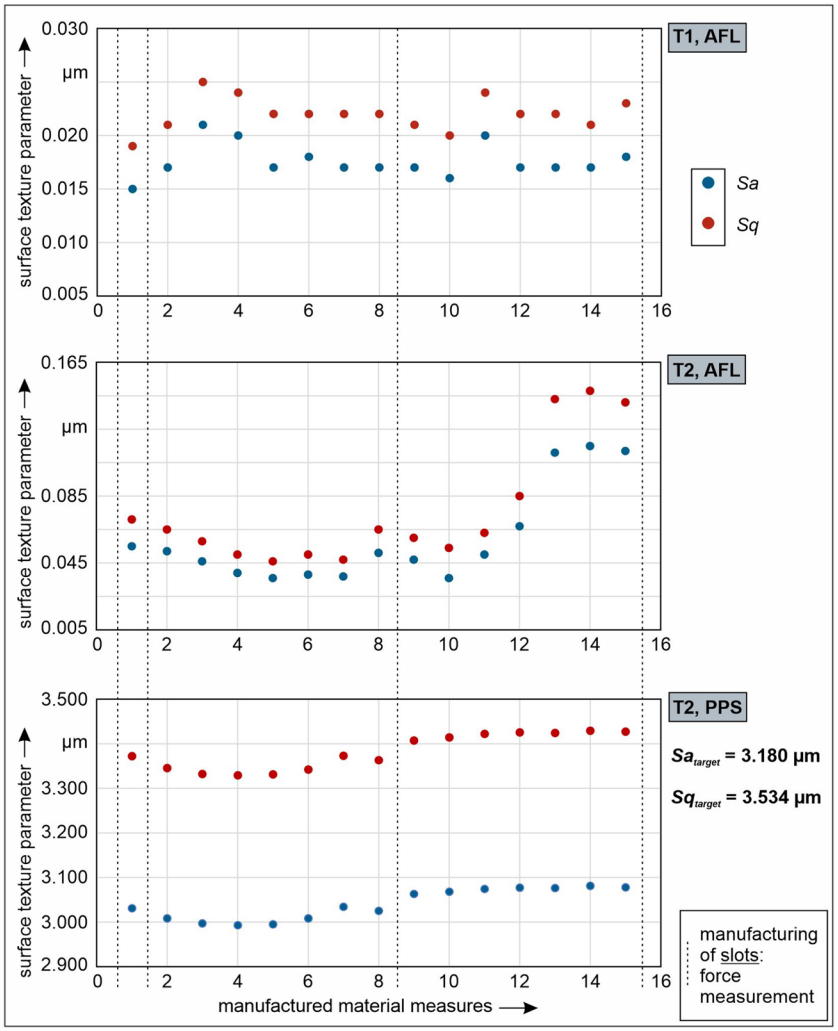

Fig. 5 Arithmetic mean values of surface texture parameters Sa and Sq over the number of manufactured material measures [3]; standard deviations are listed in Table 5 in the Appendix and are in the value range of 0.000–0.007 µm

(corresponding to the transition of the measured force values between the manufactured slots S3 and S4), which have a geometry suitable for cutting, have developed. The lowering of the forces and the constant quality of the topographies suggest that the wear caused by the built-up edge is stagnating. However, the constant course of the surface texture parameters is a stochastic behavior, which cannot be predicted with certainty. It must be considered that the adhesions or built-up edges on the cutting edge can grow or break away at any time, which is why the tool should still be changed in order to minimize stochastic influences on the process result.

4.3 Tool wear: SEM image analysis

The SEM images are used to verify the statements made about the state of the cutting edges and possible built-up edges as described in Sect. 4.2. It must be noted, however, that the SEM images are always only a snapshot at the time of the process interruption.

Figure 6 summarizes the SEM images of T1, T2 AFL, and T2 PPS for the four time steps before test 1 and after the tests 1, 2, and 3, i.e., the new tool, the tool after the manufacturing of two slots and one material measure (test 1), after overall three slots and eight material measures (test 2), and after overall four slots and 15 material measures (test 3) (see Table 3). No abrasive wear can be detected on the cutting edge of tool T1 with the SEM used (see Fig. 6) when the qualitative analysis is performed. The cutting edge appears ideally sharp. Adhesions on the rake face of the tool can already be detected before test 1 (new tool). These probably originate from the manufacturing process of the tool (grinding) and could not be removed in an ultrasonic bath with isopropanol (duration 3 min). Since the adhesions are far enough away from the cutting wedge, which is engaged during machining, they have no influence on the process result. No changes with regard to the cutting edge can be detected between test 2 and test 3 either. The minimal changes in the force signal over feed travel can therefore not be verified on the basis of the SEM images.

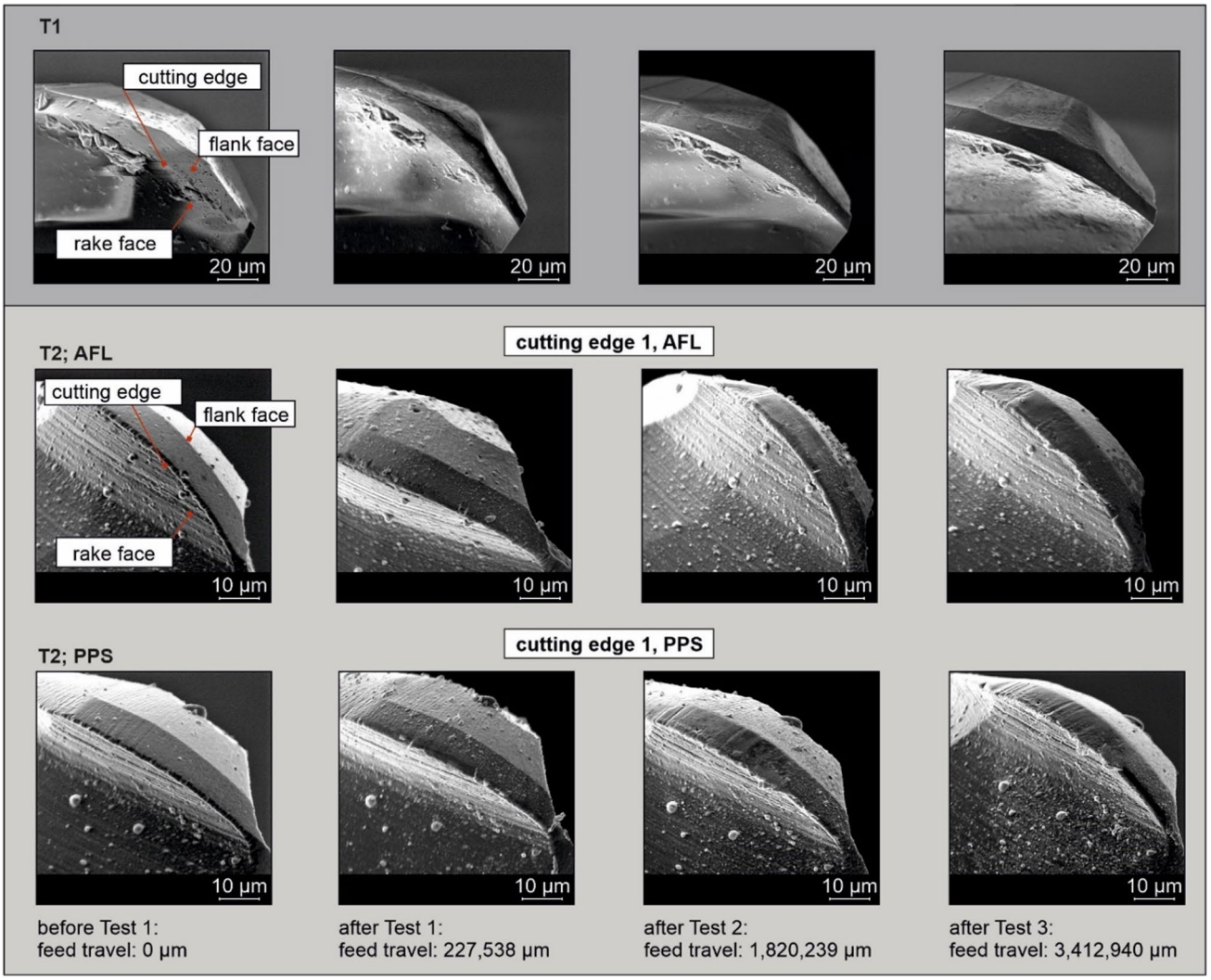

Fig. 6 SEM images of the different tools und feed travels [3]

For both geometries (AFL and PPS), it was determined from the SEM images for the tools T2 that the wear occurred mainly on one cutting edge (cutting edge 1) of the two fluted milling tool. The respective second cutting edges are shown in Fig. 7. With two fluted micro-milling tools, there is always the risk that the two cutting edges are arranged eccentrically due to smallest manufacturing deviations and are not equally involved in the cutting process. When manufacturing the material measures, only very small feeds per tooth are set (see Table 1), which is why it is possible that only one cutting edge was engaged during milling.

No major changes could be identified between the unused tool and the tool after test 1 based on the SEM images for the AFL geometry (see Fig. 6). After test 2, adhesions could be detected at the cutting edge. The adhesions were even more prominent after test 3. These adhesions, which remain on the tool despite cleaning in the ultrasonic bath (3 min with isopropanol), change during the cutting process and grow further or partially break off again. Such changes became clear in the force signal.

The tool wear for tool T2, with which the PPS geometry was manufactured, showed very similar wear behavior over the tool life investigated. However, the first built-up edge could already be detected after test 1. Furthermore, with increasing tool life, larger built-up edges became visible than for the tool with which the AFL geometry was manufactured. Due to the bigger resultant forces, the earlier onset of wear can be verified. The decreasing resultant forces between S3 and S4 cannot be explained based on the SEM images after test 2 and test 3. However, since adhesions were present, it can be assumed that these have led to the decrease in resultant forces by changing their shape and leading to a sharper cutting edge.

Based on the described tests and the evaluated parameters, the following recommendations for the two tools can be derived:

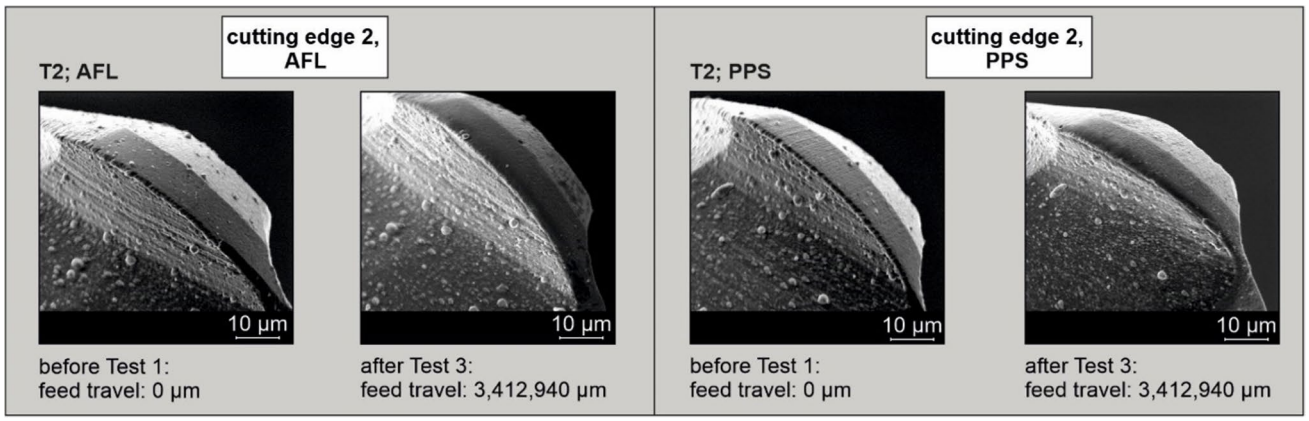

Fig. 7 Second cutting edge without wear for the two fluted tool T2 [3]

4.3.1 T1

In summary, for tool T1, the resultant forces increase from test 2. This increase is probably due to abrasive wear on the cutting edge. However, the shape deviation of the cutting edge is so small that it could not be identified with the SEM used. The surface texture parameters of 15 manufactured material measures mostly differ only in the single-digit nanometer range and do not exhibit any systematic trend. Based on the tests carried out, it can be assumed that a manufacturing of 15 material measures in brass CuZn39Pb3 with a diamond ball-end micro-milling tool can be classified as uncritical and can be performed in practice without replacing the tool.

4.3.2 T2

For tool T2, more significant tool wear occurred than for tool T1. The wear can be identified from the recorded process forces as well as from the SEM images and evaluated surface texture parameters. Accordingly, when using the tools from type T2, it is important that the critical tool life is not exceeded, because otherwise the quality of the manufactured material measures will be affected as it could be shown that for example after the manufacturing of 12 type AFL material measures, the resulting surface texture parameters change notably. For both types of material measures AFL and PPS investigated, the critical tool life is approximately ten manufactured calibration fields. After that, the tool should be replaced.

5 Conclusion

For the detection of tool wear on micro-milling tools, different methodologies were applied and compared. These methods have been examined for the general determination of tool wear in the applied manufacturing process. In the present study, the consequences for the application of the manufacturing method for material measures were examined.

Overall, the described tests have shown that the investigation of the resultant force is a very sensitive method for the detection of tool wear. However, it must be considered that the recorded forces, especially for tool T1, were in the same order of magnitude as the measurement noise. Very small changes within the process forces must therefore be critically verified. In addition, when adhesions occur, they can change their geometric shape over the tool life and cause the resultant forces to decrease again.

SEM images offer the possibility of examining the wear qualitatively in great detail. However, a process interruption is necessary and therefore there is always only the possibility of a snapshot. Particularly in the case of built-up edges with varying shape over the tool life, snapshots offer only an inadequate opportunity to predict further wear behavior.

Ultimately, the evaluation of the relevant surface texture parameters to be calibrated is of course the decisive criterion for assessing the quality of the manufactured material measure. However, the measurement can only be carried out after the material measure has been completely manufactured.

The challenges posed by the small micro-milling tools and the respective limitations of the individual measurement methods can be met by combining the measurement methods described. In practice, therefore, a qualitative evaluation of the tools by means of SEM should be carried out before the manufacturing of the material measures and the process force should be recorded and displayed during machining. However, with the approach described, it is possible to investigate how many material measures can be milled with one tool for different tool-material-topography combinations. Thus, a consistent quality of the material measures can be guaranteed and the maximum tool life can still be utilized. The utilization of the tool life contributes to cost reduction as well as to the sustainability of the process.

Appendix

Table 5 Mean value and empirical standard deviations of surface texture parameters [3]

Tool	Manufactured material measure	Mean value of Sa (μm)	Empirical standard deviation of Sa (μm)	Mean value of Sa (μm)	Empirical standard deviation of Sq (μm)
T1, AFL	1	0.015	0.000	0.019	0.000
	2	0.017	0.000	0.021	0.000
	3	0.021	0.000	0.025	0.000
	4	0.020	0.000	0.024	0.000
	5	0.017	0.000	0.022	0.000
	6	0.018	0.000	0.022	0.000
	7	0.017	0.000	0.022	0.000
	8	0.017	0.001	0.022	0.001
	9	0.017	0.000	0.021	0.000
	10	0.016	0.000	0.020	0.000
	11	0.020	0.000	0.024	0.000
	12	0.017	0.000	0.022	0.000
	13	0.017	0.000	0.022	0.000
	14	0.017	0.000	0.021	0.000
	15	0.018	0.000	0.023	0.000
T2, AFL	1	0.055	0.001	0.071	0.001
	2	0.052	0.000	0.065	0.000
	3	0.046	0.000	0.058	0.000
	4	0.039	0.000	0.050	0.000
	5	0.036	0.000	0.046	0.000
	6	0.038	0.000	0.050	0.000
	7	0.037	0.000	0.047	0.000
	8	0.051	0.000	0.065	0.000
	9	0.047	0.000	0.060	0.000
	10	0.036	0.000	0.054	0.002
	11	0.050	0.000	0.063	0,000
	12	0.067	0.000	0.085	0.000
	13	0.111	0.006	0.143	0.007
	14	0.115	0.000	0.148	0.001
	15	0.112	0.001	0.141	0.001
T2, PPS	1	3.031	0.003	3.372	0.004
	2	3.008	0.001	3.345	0.001
	3	2.997	0.003	3.332	0.003
	4	2.993	0.001	3.329	0.001
	5	2.995	0.002	3.331	0.002
	6	3.008	0.002	3.342	0.002
	7	3.034	0.002	3.373	0.002
	8	3.025	0.003	3.363	0.003
	9	3.063	0.001	3.407	0.002
	10	3.068	0.001	3.414	0.001
	11	3.074	0.004	3.422	0.004
	12	3.077	0.001	3.425	0.002
	13	3.076	0.003	3.424	0.003
	14	3.081	0.002	3.429	0.003
	15	3.078	0.002	3.427	0.002

Author contribution Katja Klauer-Dobrowolski: conceptualization, methodology, experiments, analysis, and writing—original draft.
Matthias Eifler: conceptualization, methodology, analysis, and writing—original draft.
Benjamin Kirsch: conceptualization, project administration, writing—review and editing, and supervision.
Jörg Seewig: conceptualization, supervision, and funding acquisition.
Jan C. Aurich: conceptualization, supervision, and funding acquisition.

Funding Open Access funding enabled and organized by Projekt DEAL. This work was funded by the Deutsche Forschungsgemeinschaft (DFG, German Research Foundation)—project number 172116086-SFB 926.

Declarations

Conflict of interest The authors declare no competing interests.

Disclaimer Naming of specific manufacturers is done solely for the sake of completeness and does not necessarily imply an endorsement of the named companies nor that the products are necessarily the best for the purpose.

Open Access This article is licensed under a Creative Commons Attribution 4.0 International License, which permits use, sharing, adaptation, distribution and reproduction in any medium or format, as long as you give appropriate credit to the original author(s) and the source, provide a link to the Creative Commons licence, and indicate if changes were made. The images or other third party material in this article are included in the article's Creative Commons licence, unless indicated otherwise in a credit line to the material. If material is not included in the article's Creative Commons licence and your intended use is not permitted by statutory regulation or exceeds the permitted use, you will need to obtain permission directly from the copyright holder. To view a copy of this licence, visit http://creativecommons.org/licenses/by/4.0/.

References

1. Nemoto K, Yanagi K, Aketagawa M, Yoshida I, Uchidate M, Miyaguchi T, Maruyama H (2009) Development of a roughness measurement standard with irregular surface topography for improving 3D surface texture measurement. Meas Sci Technol 20:084023
2. Leach R, Giusca C, Rickens K, Riemer O, Rubert P (2014) Develeopment of material measures for performance verifying surface topography measuring instruments. Surf Topogr Metrol Prop 2:025002
3. Klauer K (2022) Mikrofräsen flächenhafter Kalibriernormale auf Basis realer Bauteiloberflächen. Dissertation, Technische Universität Kaiserslautern: Kaiserslauten
4. Denkena B, Tönshoff HK (2011) Spanen – Grundlagen. 3, bearbeitete und erweiterte Auflage, 3rd edn. Springer-Verlag, Berlin, Heidelberg
5. Dimla E, Dimla S (2000) Sensor signals for tool-wear monitoring in metal cutting operations – a review of methods. Int J Mach Tools Manuf 40(8):1073–1098
6. Klocke F (2018) Fertigungsverfahren 1 – Zerspanung mit geometrisch bestimmter Schneide, 9th edn. Springer Vieweg, Berlin
7. Cheng K, Huo D (eds) (2013) Micro-cutting – fundamentals and applications. Wiley, Hoboken
8. Zhang C, Zhang J (2013) On-line tool wear measurement for ball-end milling cutter based on machine vision. Comput Ind 64(6):708–719
9. Fernández-Robles L, Sánchez-González L, Díez-González J, Castejón-Limas M, Pérez H (2021) Use of image processing to monitor tool wear in micro milling. Neurocomputing 452:333–340
10. Li X (2002) A brief review – acoustic emission method for tool wear monitoring during turning. Int J Mach Tools Manuf 42(2):157–165
11. Byrne G, Dornfeld D, Inasaki I, Ketteler G, König W, Teti R (1995) Tool condition monitoring (TCM) – the status of research and industrial application. Ann CIRP 44(2):541–567
12. Malekian M, Park SS, Jun MBG (2009) Tool wear monitoring of micro-milling operations. J Mater Process Technol 209:4903–4914
13. Oliaei SNB, Karpat Y (2015) Influence of tool wear on machining forces and tool deflections during micro milling. Int J Adv Manuf Technol 84:1963–1980
14. Lamraoui M, Thomas M, El Badaoui M (2014) Cyclostationarity approach for monitoring chatter and tool wear in high speed milling. Mech Syst Signal Process 44(1–2):177–198
15. Stavropoulos P, Papacharalampopoulos A, Vasiliadis E et al (2016) Tool wear predictability estimation in milling based on multi-sensorial data. Int J Adv Manuf Technol 82:509–521
16. Niu Z, Jiao F, Cheng K (2018) An innovative investigation on chip formation mechanisms in micro-milling using natural diamond and tungsten carbide tools. J Manuf Proc 31(1):382–394
17. Zhang X, Yu T, Zhao J (2020) Surface generation modeling of micro milling process with stochastic tool wear. Precis Eng 61:170–181
18. Zhang X, Yu T, Dai Y, Qu S, Zhao J (2020) Energy consumption considering tool wear and optimization of cutting parameters in micro milling process. Int J Mech Sci 178:105628
19. Zhang X, Yu T, Xu P, Zhao J (2022) In-process stochastic tool wear identification and its application to the improved cutting force modeling of micro milling. Mech Syst Signal Process 164:108233
20. Zhu K, Wong YS, Hong GS (2009) Multi-category micro-milling tool wear monitoring with continuous hidden Markov models. Mech Syst Signal Process 23:547–560
21. Alhadeff LL, Marshall MB, Curtis DT, Slatter T (2019) Protocol for tool wear measurement in micro-milling. Wear 420–421:54–67
22. Rahman M, Kumar AS, Prakash JRS (2001) Micro milling of pure copper. J Mater Process Technol 116:39–43
23. Zhu K, Yu X (2017) The monitoring of micro milling tool wear conditions by wear area estimation. Mech Syst Signal Process 93:80–91
24. Schaller Th, Bohn L, Mayer J, Schubert K (1999) Microstructure grooves with a width of less than 50 µm cut with ground hard metal micro end mills. Precis Eng 23:229–235
25. Kious M, Ouahabi A, Boudraa M, Serra R, Cheknane A (2010) Detection process approach of tool wear in high speed milling. Measurement 43(10):1439–1446
26. Klauer K, Eifler M, Kirsch B, Seewig J, Aurich JC (2020) Micro milling of areal material measures – study on surface generation for different up and down milling strategies. Procedia CIRP 87 - Proc 5th CIRP Conf Surf Integr, pp 13–18
27. Klauer K, Eifler M, Kirsch B, Seewig J, Aurich JC (2019) Correlation between different cutting conditions, surface roughness and dimensional accuracy when ball end micro milling material measures with freeform surfaces. Mach Sci Technol 24(3):446–464
28. ISO 25178–70 (2014) Geometrical product specifications (GPS)—surface texture: areal—part 70: material measures (ISO 25178–70:2014)

29. Reichenbach IG (2017) Beitrag zur Beherrschung der Mikrofräsbearbeitung von Polymethylmethacrylat. Dissertation, Technische Universität Kaiserslautern: Kaiserslautern
30. ISO 16610–61 (2016) Geometrical product specification (GPS) – filtration – part 61: linear areal filters: Gaussian filters (ISO 16610–61:2015)
31. ISO 25178–2 (2012) Geometrical product specifications (GPS) – surface texture: areal – part 2: terms, definitions and surface texture parameters (ISO 25178–2:2012)

Publisher's note Springer Nature remains neutral with regard to jurisdictional claims in published maps and institutional affiliations.

This article is a comprehensive edition of experimental results published in a PhD thesis in German language:

[3] Klauer K (2022) Mikrofräsen flächenhafter Kalibriernormale auf Basis realer Bauteiloberflächen. Dissertation, Technische Universität Kaiserslautern.